

Simultaneous X-ray absorption and two-photon LIF for imaging the spray formation region

D. Guénot¹, O. Lundh¹, K. Svendsen¹, J. Björklund Svensson¹, M. Hansson¹, I. G. Gonzáles¹, H. Ekerfelt¹, A. Persson¹, E. Berrocal^{1*}.

Department of Physics, Lund University, PO Box 118, SE-22100, Lund, Sweden.

*Corresponding author: edouard.berrocal@forbrf.lth.se

Abstract

Imaging the spray formation region of atomizing sprays is particularly challenging due to the presence of a variety of irregular liquid structures such as ligaments, liquid blobs, droplets, liquid sheets and a possible liquid core. The number and concentration of those liquid bodies dictate the presence of liquid/air interfaces, which are responsible to undesired scattering effects. The resulting images are blurred, ultimately concealing the real structure of the spray formation region. Due to both, scattering effects and the presence of highly irregular 3D liquid structures, the only reliable measurement of liquid mass in the spray formation region is obtained using X-ray radiography. The generation of collimated X-rays pulsed has been done, in the past, by means of a synchrotron, thus limiting the number of studies that can be performed.

In parallel to the use of X-rays, progresses in advanced laser imaging techniques for suppressing multiple scattering issues have been particularly important over the past decade. A very recent solution consists in using 2-photon excitation LIF laser sheet imaging.

In this paper, we report for the first time the possibility of simultaneously imaging an atomizing spray using X-ray absorption and 2-photon LIF planar imaging, where the simultaneous single-shot recordings are made over a ~20mmx20mm viewed area. The spray is generated from a commercial fuel port injection system from which, water was injected. The unique illumination/detection scheme proposed here was made possible thanks to the use of X-rays emitted from a laser plasma accelerator (Betatron radiation). For this experiment, we use the High Intensity Laser system at Lund University that provides on target 800mJ, 38fs laser pulses. The emitted X-ray radiation is ranging from 1 to 10keV and peaking at ~2keV. It propagates outside of the vacuum chamber where an X-ray camera records the shadow of the liquid jet. In addition to that, a fraction of the laser pulse ~10mJ is directed on the liquid jet and focuses with a cylindrical lens where it induces fluorescence from a 2-photon excitation process in a dye -here, fluorescein- added to the liquid. The 2p-LIF images provide details on the size and shape of the liquid structures, optically sectioned by the light sheet, while the integrated liquid mass is extracted from the X-ray radiography. This is making the two imaging techniques highly complementary for the characterization of spray systems as well as for further understanding the physics related to liquid atomization.

Keywords

X-ray absorption, 2-photon LIF, spray formation, fuel port injection.

Introduction

The atomization of liquid jets is a fundamental process which is used for a variety of industrial applications such as applying paints or chemicals for surface treatment, cutting material by means of water-jet cutters, cooling hot environment or surfaces, injecting ink for printers, treating crops in agriculture *etc.* However it is in the field of combustion that atomizing sprays are the most extensively used. For example, liquid fuels are injected within internal combustion engines, such Diesel and GDI (Gasoline Direct Injection) engines; requiring the exact amount of fuel to be injected, atomized and mixed prior to combustion. The combustion of kerosene in gas turbine aero engines is another very important example relying on the use of liquid jets. In parallel to the optimization of existing devices running on fossil fuels, there is a strong interest in developing flexible devices which can also run with liquid biofuels (e.g. bio-diesel, ethanol). However, the properties (e.g. liquid surface tension, viscosity, density) can significantly differ from one liquid fuel to another and changing those properties will directly impact on the atomization process, the combustion efficiency and the emission of pollutants emission. It is therefore very important to accurately characterize spray systems by means of imaging techniques in order to: 1) provide a detailed visualization of the spray formation 2) quantitatively describe the formed cloud of droplets.

One of main challenge in spray imaging is to mitigate the effects of multiple light scattering generated by the surrounding droplets, blobs and other liquid bodies which are present outside the image plane. This out-of-focus light contribution is responsible for visibility reduction and for image distortion. The efforts and means employed to overcome problems related to multiple light scattering have increased over the past two decades leading to the development and application of a variety of imaging techniques. Some approaches consist in selectively filtering out photons that have undergone multiple scattering events. This filtering can be done by time gating (e.g.

Ballistic Imaging [1-2]) and/or using spatial Fourier filtering. A second approach consists in suppressing the light intensity from multiple scattering after image recording via image post-processing. This is the case for Structured Illumination based techniques [3-6] where a spatially modulated illumination allows encoding the incident light and differencing it from the multiple scattering intensity - which is mostly non-modulated -. A third approach consists in directly reducing the generation of multiple light scattering. This can be performed by either using X-rays [7-9] where absorption is the main interaction process while scattering is negligible or by implementing two-photon laser induced fluorescence (2p-LIF) imaging as recently demonstrated in [10].

- With X-ray illumination, the refractive index of water is close to unity for photon in the keV range while its absorption cross-section is above $10^2 \text{cm}^2/\text{g}$. Thus, X-ray radiography provides a solution to suppress the occurrence of scattered radiations and has been successfully employed for various spray studies [7-9]. However, because of the short time scale ($<1\mu\text{s}$) and the high X-ray flux that is required, most of the research effort related to radiography of transient spray systems has been accomplished through the use of a synchrotron facility, which, in addition to the cost of it, has limited availability. Furthermore, the X-ray beams generated by synchrotron presents a number of drawbacks: First they have a small divergence ($<1\text{mrad}$) requiring long beam transport lines and leading to narrow imaged areas (only a few mm). In addition, because of the high photon energy ($> 5\text{keV}$) a contrast agent (e.g. potassium iodide, KI) is inserted in the injected liquid, up to a non-negligible concentration. It has been shown in [11,12] that such additives changes the liquid viscosity and thus modify the entire atomization process. Despite those drawbacks, X-ray radiography is the most reliable solution to measure liquid mass distribution in the near-nozzle region where the spray is being formed. In comparison, visible radiation can obtained the extinction coefficient from transmission measurement only if: 1) the droplets are already formed and spherical -in the spray region-, 2) if enough non-scattered photons are still crossing the spray -optical depth inferior than ~ 6 -; 3) if multiple light scattering is suppressed [13].

- The advantage of 2p-LIF detection in optically dense sprays is that it provides higher visibility than for any other detections schemes such as one photon liquid LIF or elastic Mie scattering [10]. The main reason for that is that photons which undergo multiple scattering processes spread in space and time, making the probability of having two photon simultaneously absorbed highly reduced. On the contrary, at the location where the illuminating light sheet is focused the probability for the 2p-LIF process to occur at its highest; providing a signal that is only generated at the object plane of the camera objective.

In this article, we are aiming at imaging disintegrating liquid jets -generated from a port fuel injection system using simultaneously X-ray radiography and 2p-LIF light sheet imaging. We make this challenging configuration possible by using a laser plasma accelerator; a technique that has been initially developed in the early years 2000 [14]. It consists in focusing an intense femtosecond laser pulse into a gas jet, to accelerate electrons to hundreds of MeV and to generate X-rays in the keV range. The main advantage of the approach is that it provides ultra-short X-ray pulses through a collimated beam of fairly large dimension (beam diameter in the cm range) which is much larger than what synchrotron facilities usually provide (beam diameter in the mm range). In addition X-rays of lower energy can be generated (from 2 to 10 keV), increasing absorption sensitivity. Finally, as the approach is based on using femtosecond laser pulses; a portion of it can easily be used to simultaneously image the spray using 2p-LIF at no extra cost. The presented simultaneous imaging configuration is applied on water liquid jets, generated by a commercially available port fuel injection system, at different time (from $50 \mu\text{s}$ to $1150 \mu\text{s}$) after the visible start of injection.

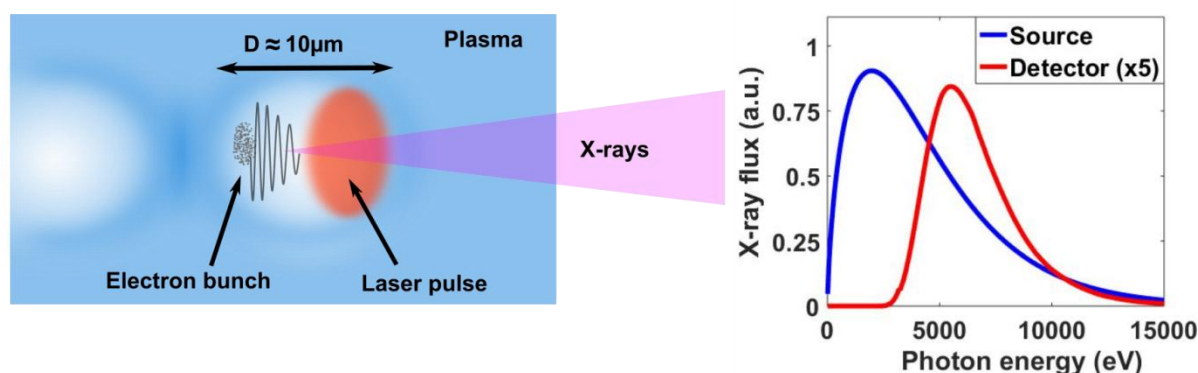


Figure 1. Scheme of the Laser plasma X-ray generation, in blue is the background plasma density, in red is the laser pulse and in purple is the X-ray beam. The inset shows the X-ray spectrum at the generation point and at the detector.

Experimental setup

The concept of accelerating electrons using a laser generated plasma was published for the first time in 1979 [14]. However, it took more than 20 years and the advent of intense femtosecond pulse to see its first experimental demonstration [16,17,18]. In this scheme, a 900mJ, 38fs laser pulse is focused down to 13 μ m onto a gas jet to reach 10¹⁹W/cm². At this intensity, the laser pulse fully ionize the gas and the ponderomotive force repels the electrons ahead of it. Therefore, if the pulse focal spot size and duration match the plasma frequency, a cavity empty of electrons will form behind the laser. In this cavity, electrons sees a strong focusing and accelerating gradient (up to 100's of GeV/m) which allow accelerating in a few millimeter electron bunches with energies around 100MeV and 5mrad divergence. During their acceleration, the electrons oscillate transversally inside the cavity; this motion leads to the generation of X-rays in the forward direction. This radiation is often referred to as the betatron radiation [16]. The emitted X-rays have a characteristic betatron spectrum described by:

$$\frac{d^2I}{d\omega d\Omega} = N_b \frac{3e^2}{2\pi^2c} \gamma_{x0}^2 \left(\frac{E}{E_c}\right)^2 \kappa_{\frac{2}{3}}^2 \left(\frac{E}{2E_c}\right)$$

With N_b the electron number, e the electric charge, c the speed of light, γ the Lorentz factor, $\kappa_{2/3}$ the modified Bessel function, E the photon energy and E_c the critical energy. E_c is typically of a few keV (2.36keV in this experiment) about 10⁹ photons are emitted, with a divergence of a few tens of mrad (20) and the bunch duration has been estimated to be of tens of femtosecond in numerical simulation. In our experiment, because of the various filters on the way (Al, Kapton, and Beryllium) the low energy photons are absorbed such that the spectrum at the detector extends from 2 to 10 keV and only 10⁸ photon remains.

In order to separate the X-rays from other particle a strong magnet is placed after the gas jet to deflect the electrons which then hit a lanex screen and induces fluorescence (see Figure2), the position on the lanex screen is recorded which allows to determine the electron beam energies. The laser beam is blocked at the end of the vacuum chamber by a 3 μ m thick Al foil. The X-ray beam crosses outside the vacuum chamber a liquid jet ejected from a commercially available fuel port injector with 4.5 bars of pressure. The liquid jet was either made of pure water either of water w 10% KI (potassium iodide) that has a higher x ray absorption. A 4 Megapixel X-ray camera (13.5 μ m size that corresponds to 11.4 μ m including magnification) recorded the absorption caused by the liquid jet. From this signal the quantity of liquid mass crossed can be inferred. The liquid jet is exiting four holes of a commercially available fuel port injector (Bosch EV1 fuel injector 4 hole nozzle).

In parallel to this, a small fraction of the beam (around 10mJ) was re-directed using a small mirror and focused by a cylindrical lens onto the liquid jet. A fluorescent dye (fluorescein) was added to the jet (0.1%) so that the 800nm laser pulsed induced two photon fluorescence at 6-500 nm. A camera placed vertically recorded the fluorescence signal simultaneously to the X-ray signal.

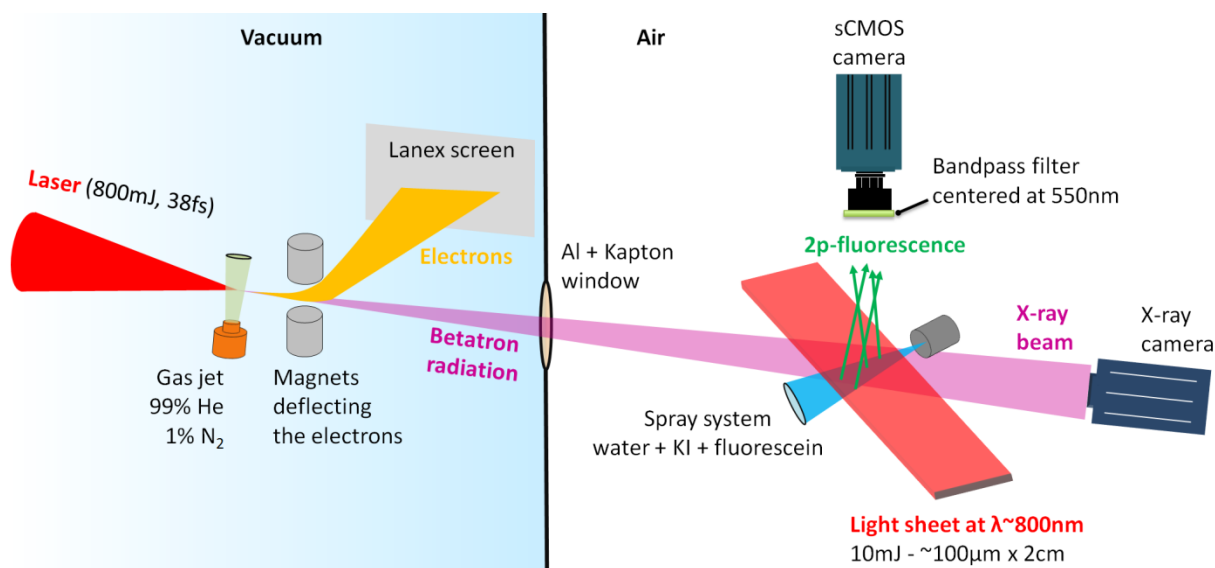


Figure 2. Illustration of the experimental setup: X-ray camera was recording the transmitted Betatron radiation while a sCMOS camera was simultaneously recording the fluorescence generate from a two photon excitation process.

Two-photon induced fluorescence imaging is a method newly introduced for the observation of liquid jets. It uses the fact that only two-photon absorption can excite the dye to get rid of the laser scattering before it interacts with the dye. This strongly limits the amount of aberration caused by the jet structures and allows imaging the jet with great spatial resolution. These two imaging techniques provide, thus, complementary information and enables to access the full spray picture both in terms of shape/structure as in terms of liquid mass distribution.

Finally, as a mean to provide a comparison with more standard technique two other optical techniques have been applied: Light sheet Mie scattering and shadowgraphy. Mie scattering from the light sheet was recorded simultaneously as the X-ray and 2p-LIF images using another camera placed vertically with a filter at 800nm in order to record only the laser scattering on the droplets and filter out the fluorescence. The shadowgraphic images have been recorded after the experiment using a frequency doubled 532nm YAG laser in similar conditions than during the experiment

Results and discussion

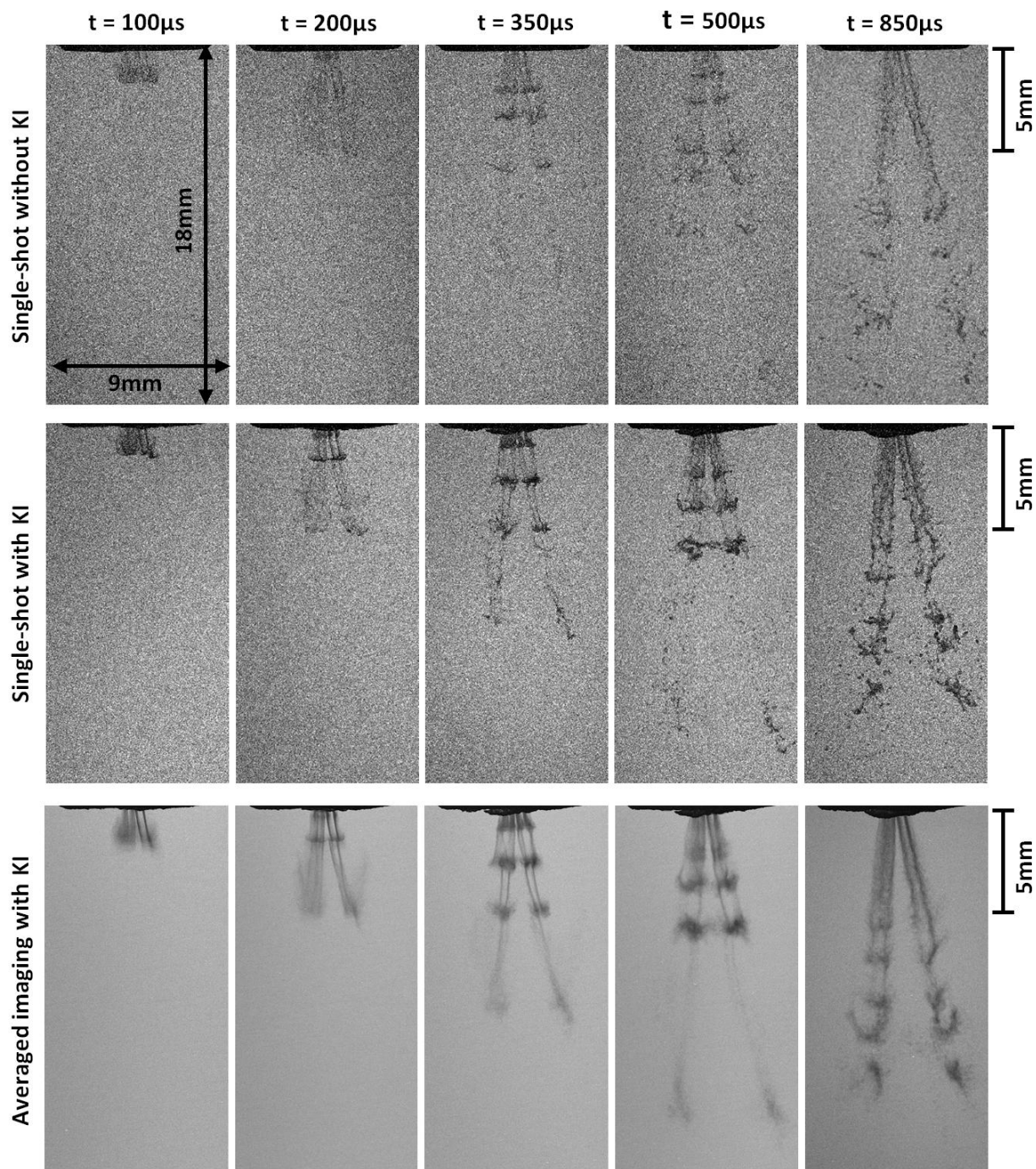


Figure 3. Raw X-ray images taken at different times after the start of injection and with different liquid mixture or different number of acquisition. The scale is the same for all images.

Figure 3 shows the measured radiograph at different times after the start of injection. The similarities between single shot images and average images indicates that the liquid jet break up structures do not significantly changes from one injection to the other. It is thus possible to average images in order to reduce noise. One clearly sees that the characteristic “sac” leads the jet; this volume comes from the liquid trapped between the valve and the final orifice and does not undergo strong turbulence. 200 μ s after the “sac” comes large breakup structures that slowly damps until the flow becomes continuous and reach a steady state after about 500 μ s.

As a mean of comparison with optical techniques, we recorded simultaneously images of the 2p-LIF as well as the Mie scattering induced by the laser light sheet. In addition to this, optical shadowgraphy images were recorded with the same conditions later on. Figure 4 shows the comparison between these images. The 2p-LIF images allows not only observing the liquid jet structure with much higher resolution (8 μ m/pixel) than with the X-ray camera but in addition to that, the light sheet allows to select only one of the jet. The images have a large noise due to the ionizing radiation generated when the accelerated electrons hit the fluorescence screen of the spectrometer. In order to limit these radiations, the camera was placed above the jet where the radiation should be lower. However, because of this configuration, the X-ray and fluorescence cameras did not observe the liquid jet from the same point of view, thus limiting our ability to compare the different images. Future experiments will require a better shielding of the camera from ionizing radiation to fix this problem.

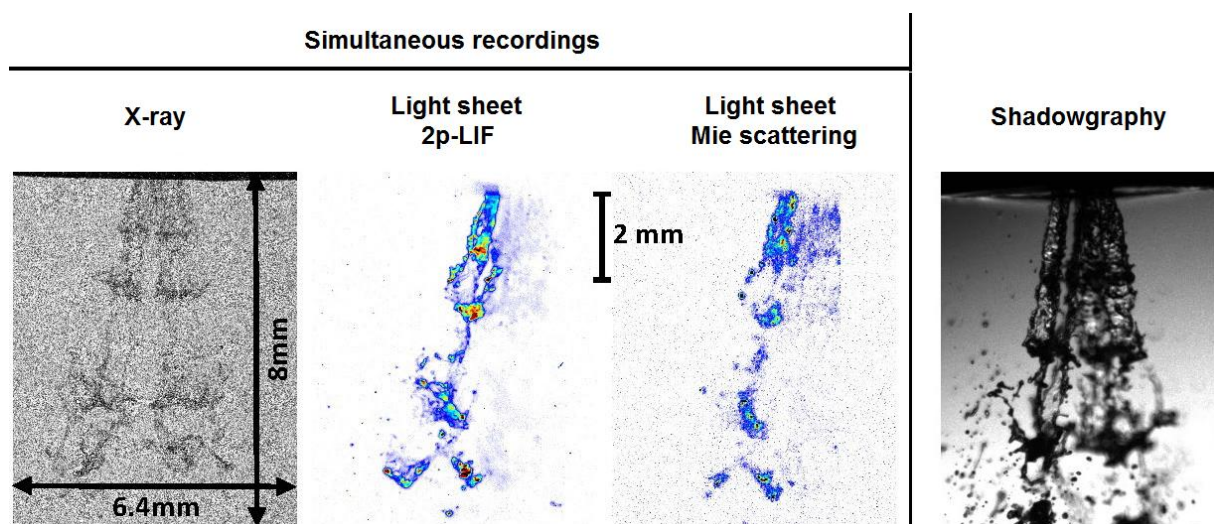


Figure 4. Zoomed images recorded by four different imaging techniques 500 μ s after the start of injection. X-ray radiography, Mie scattering and 2p-LIF images have been taken simultaneously, while the optical shadowgraphy have been recorded afterwards in the same pressure and opening conditions.

The Mie scattering image also shows various liquid bodies, however the highly non-regular structures during the liquid jet breakup some points saturates the camera due to direct reflections while the rest of the images remains at low counts. These artefacts strongly limit the measurement dynamics. The shadowgraph gives a clear representation of the entire liquid jet shape, but one cannot distinguish the depth and some parts of the images are completely dark. Finally, a major issue for performing simultaneous 2p-LIF and X-ray measurement is the effect the quenching of the dye by potassium iodide. Indeed, despite a doubling of the pump intensity, the signal decreased by an order of magnitude when using the water +10% KI mixture compare to the pure water case. In addition to that, potassium iodide changes the viscosity by about 5% when mixed with water [5,6]. This causes small changes in the liquid jet breakup dynamic that can be observed in both X-ray and fluorescence images. These problems underline the importance of having the highest signal possible in order to limit the need for contrast agent. This issue will become even more important when using other fluids such as ethanol that has an even lower X-ray absorption. In a similar way, the amount of fluorescein can also affect the properties of the injected liquid, especially for highly concentrated solutions. Figure 5 shows the variation viscosity in (a) and of the surface tension in (b) for fluorescein mixed with water. In the current experiment, 0.1% of fluorescein was used, leading to a change of 1.4% in surface tension and \sim 0.38% in viscosity. Those variations are negligible and will not affect the breakup process.

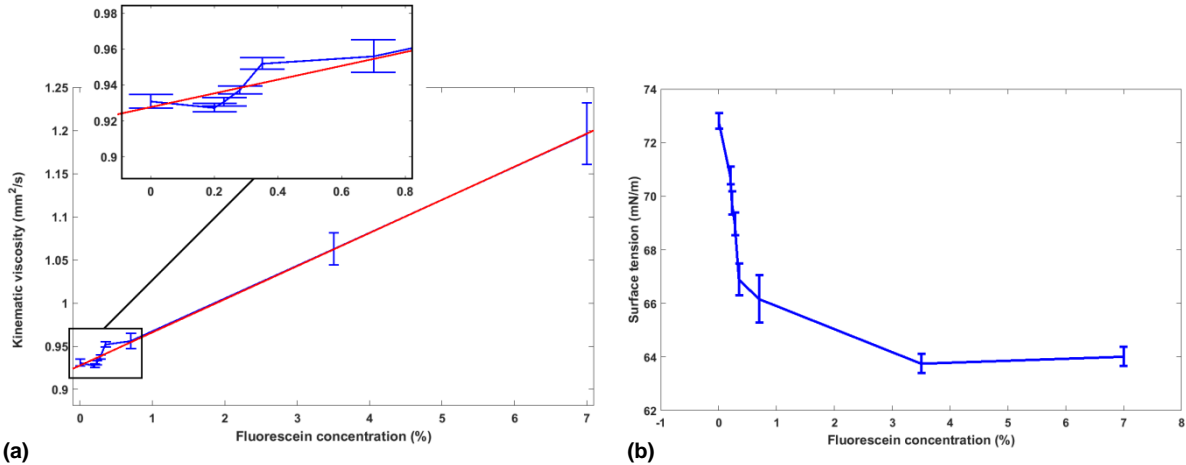


Figure 6. Variation of the water viscosity in (a) and of the water surface tension in (b) as a function of fluorescein concentration. At 0.1% fluorescein concentration, used in this experiment, it results in a 1.4% change in surface tension and ~0.38% change in viscosity which is negligible.

Calibrated X-ray results:

The most important aspect of this work is the X-ray sensitivity to water. Two aspects should be considered; the noise level and the amount of water needed to absorb X-rays. The number photon impinging the camera is estimated to $5 \cdot 10^7$, meaning that on average, around 20 photons hit each pixels in the camera thereby generating a signal to noise ratio of 3.2. Binning the camera’s pixel reduces the noise but is at the cost of spatial resolution. As an example a 3x3 binning reduces the signal to noise down to 8 at the cost that the effective pixel size is then of 34.2µm. The effective path length sensitivity is then limited by the pixel size, and thus about two times better than the latest measurement performed with synchrotron produced X-rays [19].

Figure 5, shows calibrated radiograph averaged over 50 images of the liquid jet at different times after the start of injection. This figure clearly shows where the liquid mass is statistically distributed and how the jet is evolving over time. The calibration work has been done using the curve shown in Figure 6.

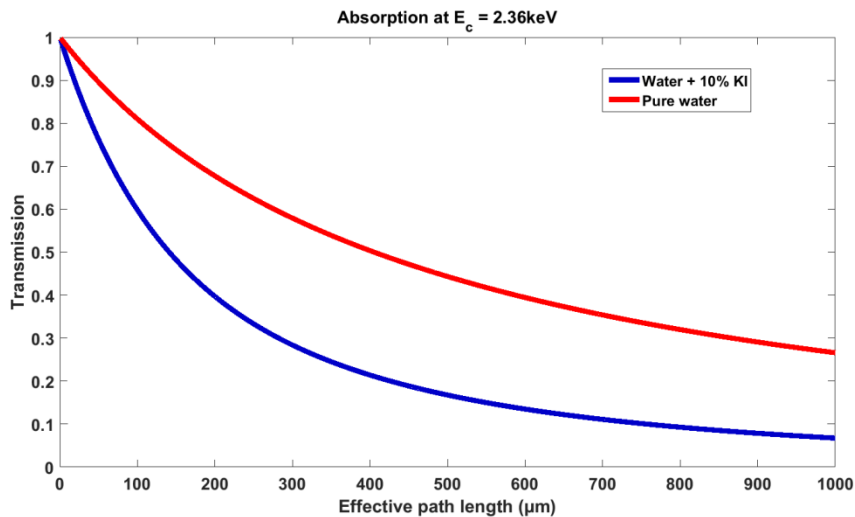


Figure 6. Transmission of 2.36 keV X-rays as a function of effective path length for pure water and a solution of water with 10% KI. Those calibration curves allows obtaining quantitative data related to liquid mass.

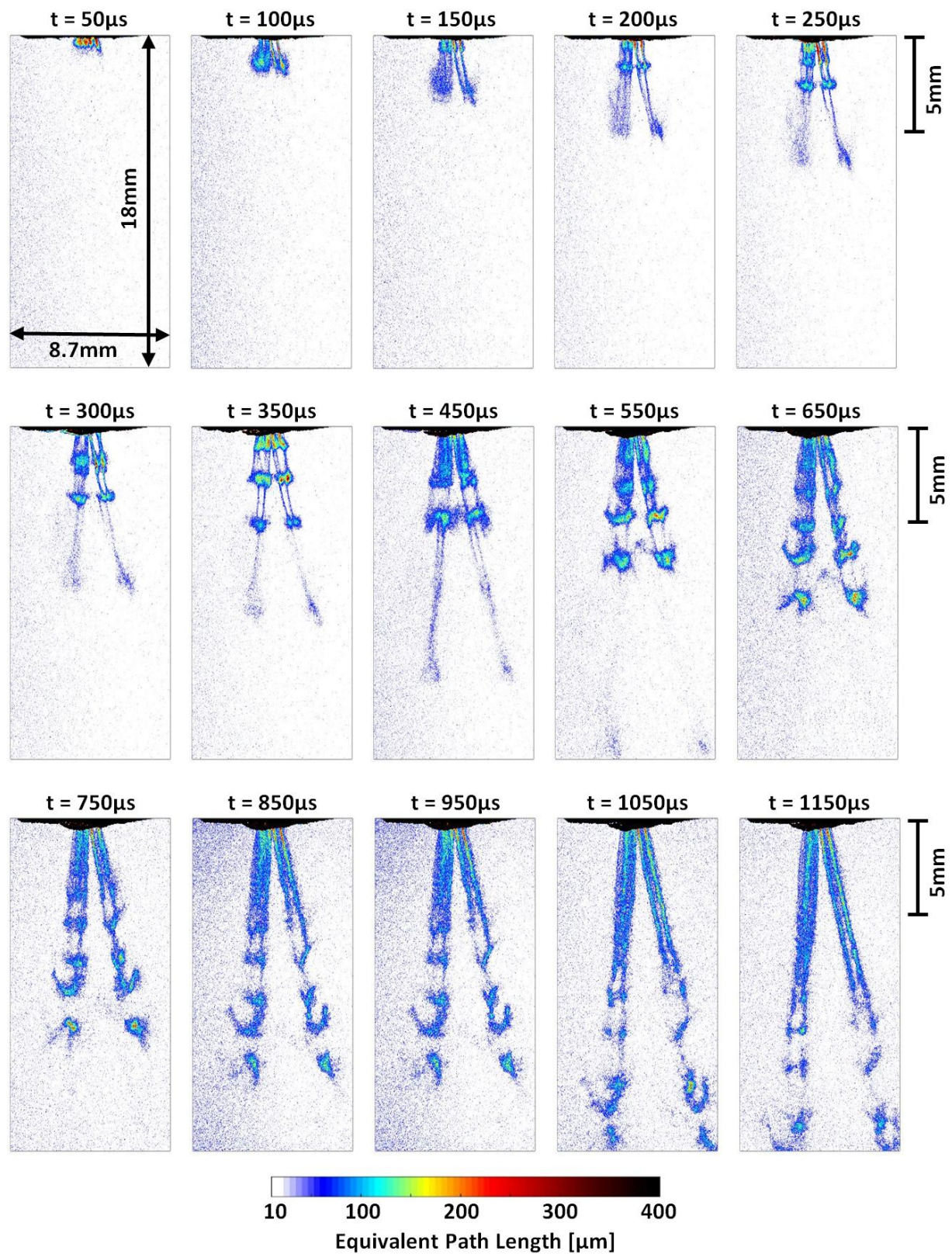


Figure 5. Calibrated X-ray images showing the equivalent path length for different time after the visible start of liquid injection. Here water is injected through a commercial port fuel injection nozzle.

Conclusion:

In order to improve the sensitivity one has to increase the absorption or decrease the signal to noise ratio. Increasing the signal to noise ratio can mostly be done by increasing the X-ray flux at the generation point and by reducing the distance between the generation point and the X-ray camera. Current improvement in the setup have led to an increase by a factor four in the X-ray signal.

As already mentioned the different filters and windows cut the lowest part of the X-ray spectrum such that at the detector, the spectrum extends from 2.5 to 12.5keV. Unfortunately, the absorption of oxygen peaks at 550eV. So an improvement of the X-ray absorption can only be achieved by reducing the mean energy of the X-rays. This requires reducing the thickness of the various filters and windows located along the X-ray path. Calculations showed that dividing by two their thickness will improve the absorption by 20%.

Acknowledgements

The European Research Council (ERC) under the European Union's Horizon 2020 research and innovation program (Agreement No. 638546—ERC starting grant "Spray-Imaging") as well as the Swedish Research Council, Vetenskapsrådet (2016-03894 and 2015-03749), and the Knut and Alice Wallenberg Foundation are acknowledged for their financial support.

References

- [1] Mark A. Linne, Megan Paciaroni, James R. Gord, and Terrence R. Meyer, "Ballistic imaging of the liquid core for a steady jet in crossflow," *Appl. Opt.* **44**, 6627-6634 (2005)
- [2] M. A. Linne, M. Paciaroni, E. Berrocal, and D. Sedarsky, "Ballistic imaging of liquid breakup processes in dense sprays," *Proc. Combust. Inst.* **32**(2), 2147–2161 (2009).
- [3] E. Berrocal, E. Kristensson, M. Richter, M. Linne, and M. Aldén, "Application of structured illumination for multiple scattering suppression in planar laser imaging of dense sprays," *Opt. Express* **16**(22), 17870–17881 (2008).
- [4] Y. N. Mishra, E. Kristensson, M. Koegl, J. Jönsson, L. Zigan, and E. Berrocal, "Comparison between two-phase and one-phase SLIPI for instantaneous imaging of transient sprays," *Exp. Fluids* **58**(9), 110 (2017).
- [5] E. Kristensson and E. Berrocal, "Crossed patterned structured illumination for the analysis and velocimetry of transient turbid media," *Sci. Rep.* **8**(1), 11751 (2018).
- [6] E. Berrocal, J. Johnsson, E. Kristensson, and M. Aldén, "Single scattering detection in turbid media using single-phase structured illumination filtering," *J. Euro. Opt. Soc. Rap. Pub.* **7**, 12015 (2012).
- [7] MacPhee, A. G. et al. "X-ray imaging of shock waves generated by high-pressure fuel sprays". *Science* **295**, 1261–1263 (2002).
- [8] C. F. Powell, S. A. Ciatti, S.-K. Cheong, J. Liu, and J. Wang, "X-ray absorption measurements of diesel sprays and the effects of nozzle geometry," *SAE Technical Paper*, (SAE International, 2004).
- [9] Benjamin R. Halls, Christopher D. Radke, Benjamin J. Reuter, Alan L. Kastengren, James R. Gord, and Terrence R. Meyer, "High-speed, two-dimensional synchrotron white-beam X-ray radiography of spray breakup and atomization," *Opt. Express* **25**, 1605-1617 (2017).
- [10] Edouard Berrocal, Chris Conrad, Jeremias Püls, Cord L. Arnold, Michael Wensing, Mark Linne, and Miguel Miranda, "Two-photon fluorescence laser sheet imaging for high contrast visualization of atomizing sprays," *OSA Continuum* **2**, 983-993 (2019).
- [11] http://chemistry.mdma.ch/hiveboard/rhodium/pdf/chemical-data/prop_aq.pdf
- [12] Söhnle, O., and Novotny, P., *Densities of Aqueous Solutions of Inorganic Substances*, Elsevier, Amsterdam, (1985).
- [13] E. Kristensson, E. Berrocal, and M. Aldén, "Quantitative 3D imaging of scattering media using structured illumination and computed tomography," *Opt. Express* **20**, 14437-14450 (2012)
- [14] Corde, S. *et al.* Femtosecond X-rays from laser-plasma accelerators. *Rev. Mod. Phys.* **85**, 0034–6861 (2013).
- [15] Tajima, T. & Dawson, J. M. Laser electron accelerator. *Phys. Rev. Lett.* **43**, 267–270 (1979).
- [16] Faure, J. *et al.* A laser-plasma accelerator producing monoenergetic electron beams. *Nature* **431**, 541–544 (2004).
- [17] Geddes, C. G. R. *et al.* High-quality electron beams from a laser wakefield accelerator using plasma-channel guiding. *Nature* **431**, 538–541 (2004).
- [18] Mangles, S. P. D. *et al.* Monoenergetic beams of relativistic electrons from intense laser-plasma interactions. *Nature* **431**, 535–538 (2004).
- [19] Halls B. R. *et al.* High-speed, two-dimensional synchrotron white-beam X-ray radiography of spray breakup and atomization. *Optics express*, **25**, 2 (2017).